Republic of Iraq
Ministry of Higher Education
and Scientific Research
University of Diyala
College of Science
Department of Physics

Preparation and study of some physical properties of Nickel doped manganese oxide films for photodetectors application

A Thesis
Submitted to the Council of the College of Science - University of Diyala in Partial Fulfillment of the Degree of M.Sc. in Physics

by

Ali Younis Ibrahim

(B. Sc. in Physics 2019)

Supervised by

Assistant Professor Dr.

Faisal Ghazi Hammoodi

2025 A.D. **1447 A.H.**

بِسْمِ اللَّهِ الرَّحْمَٰنِ الرَّحِيمِ

﴿وَيَسْأَلُونَكَ عَنِ الرُّوحِ قُلِ الرُّوحُ مِنْ أَمْرِ رَبِّي وَمَا أُوتِيتُم مِّنَ الْعِلْمِ إِلَّا قَلِيلًا ﴿٨٥﴾﴾

صدق الله العظيم

الإسراء: 85

Abstract

In this study thin films of manganese oxide (Mn_3O_4) doped with nickel oxide (NiO) with different ratios (0,1,3,5, and 7%) were prepared on glass substrates at (350 $^{\circ}$C) and with a thickness of (327) nm using the chemical spray pyrolysis, technique (CSP).

The effect of changing the nickel oxide doping ratios on the structural, optical and electrical properties of the prepared films was studied using X-ray diffraction (XRD), atomic force microscopy (AFM), field emission scanning electron microscopy (FE-SEM), UV-Visible spectroscopy and Hall effect.

The results of X-ray examinations demonstrated that all the prepared film with all different doping ratios have a polycrystalline structure of the tetragonal type and that the dominant growth orientation all films is (101). It was found that the crystal size decreases, with increasing doping ratios. The values of the lattice constants, the number of crystallites per unit area and the dislocation density were also calculated.

The results of the (AFM) showed a decrease in the mean square roughness and surface roughness with increasing nickel oxide doping ratios.

The (FE-SEM) studies revealed that the produced films have surfaces with spherical structures gathered in the shape of a flower, very similar to a cauliflower flower. However, the average grain size decreases with increasing nickel oxide (NiO) doping ratios.

The optical properties of all prepared films were studied at different doping ratios by recording the transmittance and absorbance spectra at wavelengths ranging from (300 -1100) nm. The findings demonstrated that the optical energy gap for the allowed direct electronic transition in the produced films ranges from (2.65 -2.95) eV. We note that the transmittance, values increase, while the absorbance decreases with increasing doping ratios. The optical constant were calculated for all prepared films, which include

Absorption coefficient, refractive index, extinction coefficient, and real and imaginary dielectric constant as a function of photon energy.

The produced thin films (Mn_3O_4) doped with nickel oxide at all doping ratios exhibited p-type electrical conductivity, as demonstrated by electrical testing using the Hall effect. This is because the films had low conductivity and high resistivity.

The characteristics of the detector prepared by deposition of films (Mn_3O_4) and doped (NiO) at the specified temperature and deposited on silicon substrates were studied. The results of current-voltage measurements showed that the prepared detector is of type Anisotype and that the dark and light currents increase with increasing doping ratios in the case of forward bias. However, in the case of reverse bias, a decrease in the value of the resulting current occurs with increasing doping ratios.

The detector parameters were studied, where the spectral response showed an increase with increasing doping ratios, and its highest value was at short wavelengths and in the undoped. The optical detectivity results showed a decrease with increasing doping ratios, and its highest value was at short wavelengths. The results of the output quantum efficiency increased with increasing doping ratios, and its highest value was at the pure state and at short wavelengths.

Chapter one

Introduction and Literature Review

1.1 Introduction

One of the most significant technological advancements in the study and creation of semiconductors is thin film technology, which involves one or more layers of atoms of a material with a thickness of less than (1000) nm are called thin film [1].Thin films are different in their physical properties from the properties of their constituent materials in their volumetric state as the thin Film of a particular material if we reduce its thickness very significantly to the degree of a nanometer it will be semidimensional so a change occurs to most of the physical properties of the material due to the very short distance between the limits of the two surfaces and the basic difference between the materials when they are in their thin state and their thick state is actually related to the fact that the thickness affects the physical properties it is neglected in the thick state and the films takes on the properties of the thick layer when the thickness exceeds a certain threshold [2]. In their preparation, thin films always need a base regardless of the method used to manufacture the film or thin film, although sometimes we can separate the thin film from the base. This base affects the physical properties of the deposited layer. For example, if we put two thin layers made of material on two different bases, one of which is glass and the other is silicon we will notice a significant difference in their physical properties [3]. There are many applications of thin films, including optical in the manufacture of mirrors, reflective and non-reflective coatings, as well as photocopiers and semiconductor lasers, including electronic in the manufacture and increase the efficiency of solar cells, integrated circuits and digital computers [4].Scientists have achieved substantial advancements in thin films technology for more than a century. For example, in 1852, scientists Benson and Grove successfully prepared thin metallic films using chemical reaction techniques while in 1857 Faraday employed thermal evaporation to prepare thin films. In 1876, Adams prepared a thin film of selenium in combination with platinum [5].

1.2 Thin Films Preparation Methods

Several techniques exist for thin film fabrication, each varying in precision and complexity depending on the material type and intended application [6]. The deposition method directly affects the film's physical properties. This study focuses on a simple, low-cost technique that achieves precise thickness without the need for advanced equipment [7], as illustrated in Figure (1.1).

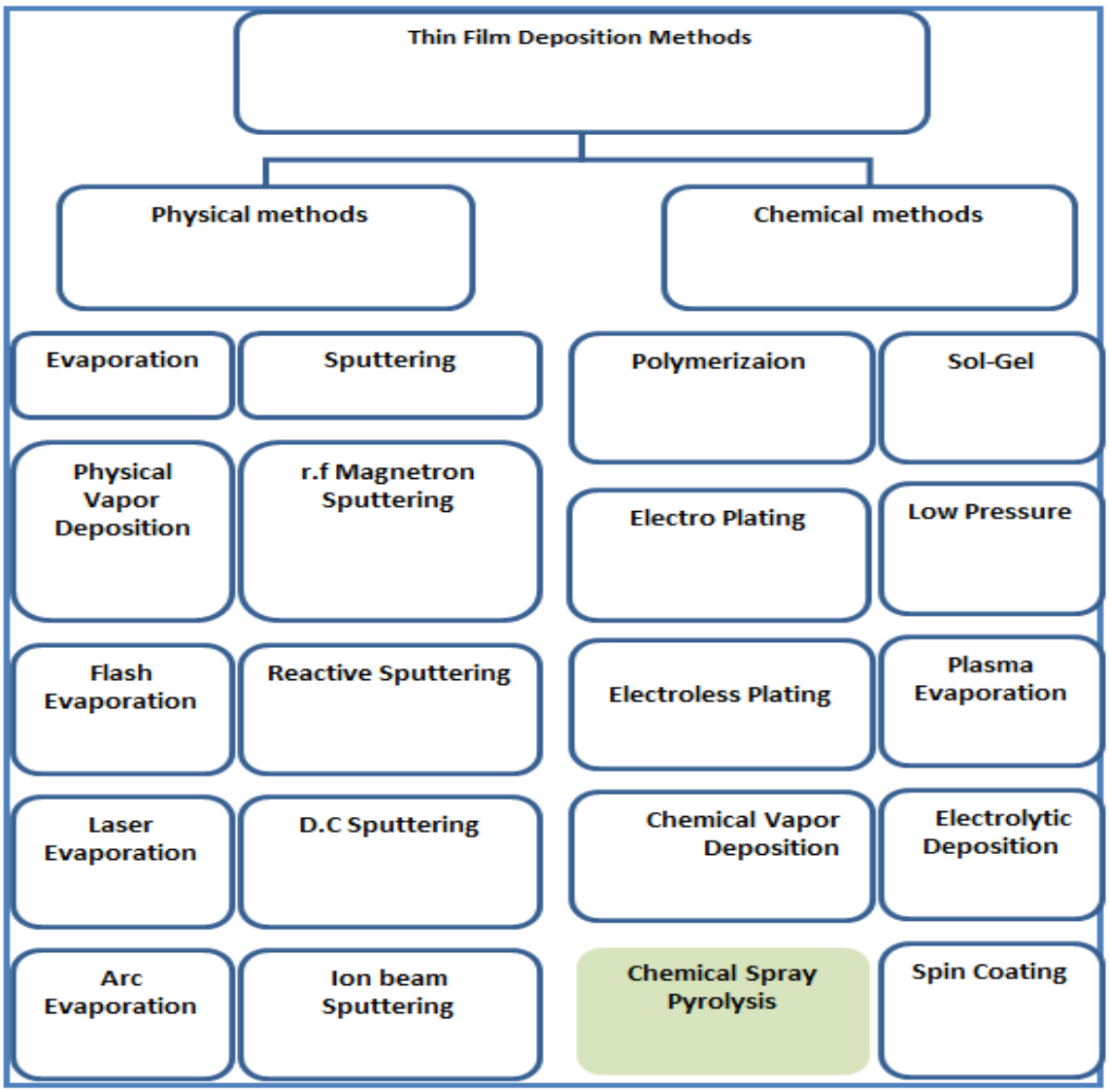

Figure (1.1): Schematic diagram of thin film Preparation methods [8]

1.3 Chemical Spray Pyrolysis Technique

There are some techniques that deposit the material on substrate, such as the chemical spray pyrolysis technique that we used in this study and it is considered one of the most widely used methods in preparing thin films. The summary of this method is to deposit a solution of the material from which the film is to be prepared on glass substrate at a temperature that depends on the type of material used in the preparation. The film prepared in this way have several advantages and the first to use this method were the researchers Hottle and Hanger[7,9] .

1. Simple and uncomplicated to use .
2. Low cost due to the availability of devices locally .
3. Films with good uniformity and large areas can be prepared .
4. It is considered a convenient method for preparing films of oxide and sulfate materials .
5. The prepared films have good adhesion to the base .

The disadvantages of this method are :

1. It takes a long time and a lot of effort to obtain the film .
2. Film cannot be prepared directly from the solid material .
3. The material from which the film is to be prepared must be in the form of a liquid .

1.4 Mechanism of Thin Films Formation

The structural composition of thin films is very complex compared to bulk materials, whether polycrystalline or single crystalline. Films generally have structures with very small grain sizes and therefore the density of grain boundaries is very large i.e. the density of defects and irregularities is much greater than that of other materials [7] .The mechanism of thin film deposition can be defined in three main steps:

1. Providing , molecules , atoms or ions to the precipitation solution of the film material.
2. Transferring it to the substrste or the part to be coated through a conveyor medium.
3. Condensing it on the base directly, chemically, physically, or by other deposition methods to form a solid precipitate.

The process of deposition of thin films is carried out first through the nucleation process i.e. The formation of nuclei on the substrate on which the thin films are built. Nuclei are formed when atoms molecules or ions move from the source to the substrate. These molecules begin to assemble and form what are called nuclei. These nuclei grow in three dimensions and this growth is more horizontally aligned with the substrate than vertically due to the surface diffusion of atoms. This is a distinctive feature of the growth of thin films [10] . The process of nuclei growth during the film deposition process is called islanding. There are several factors that affect the formation of these islands namely the temperature of the base the type of deposited material and the rate of deposition. After the process of forming the awl the small islands begin to coalesce to form grain boundaries in polycrystalline materials. They may coalesce to form a single crystal if the coalesced islands are in one direction [10, 11] . The islands continue to join together and begin to change their shape extending elongating and connecting with each other, forming narrow areas near the area of adhesion to each other. These areas are characterized by being irregular and long, called channels. When the sedimentation process continues nuclei and islands are produced within these channels, which quickly merge upon contact with the walls of the channels, forming what resembles bridges, leaving voids within the film. These channels disappear and decay, forming a continuous film by the continued formation of secondary islands that touch the edges of the vacuoles and merge with the main film [12] .

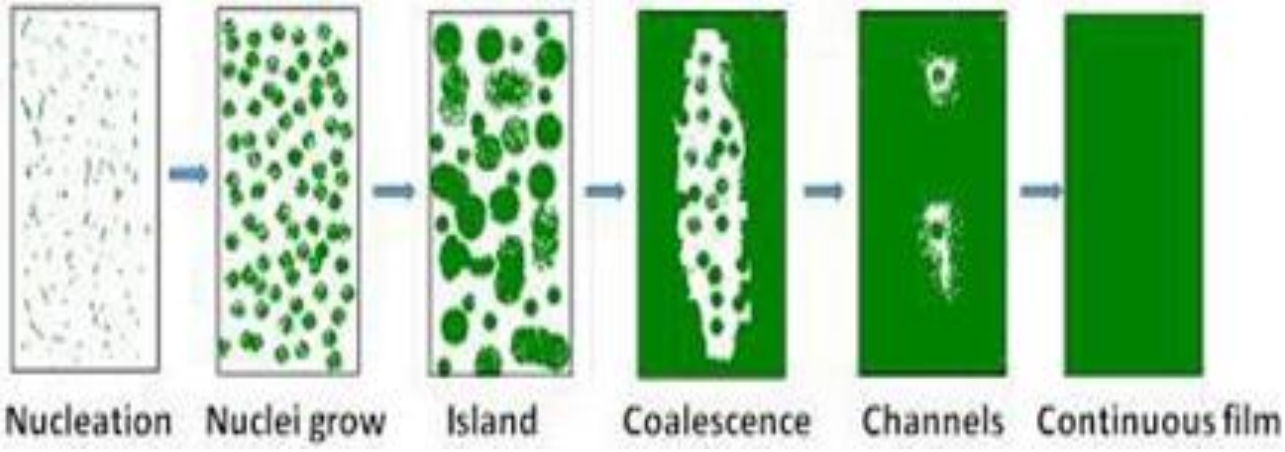

Figure (1.2) The stages of thin film formation [13]

1.5 The Drops Size Effect

The mechanism by which thin films are formed by chemical pyrolysis (CSP) methods depends on the principle of droplet collision with the substrate, as the droplets are launched from the spray device at an initial speed towards the hot substrate, where the launch process is in the form of a spray in order to obtain the largest possible amount of droplets on the substrate and the efficiency of droplet spraying must be controlled to obtain the required droplet size. There are four possible cases of decomposition depending on the size of the formed droplets[13]. Figure (1.3) shows the deposition cases depending on the size of the droplets [14].

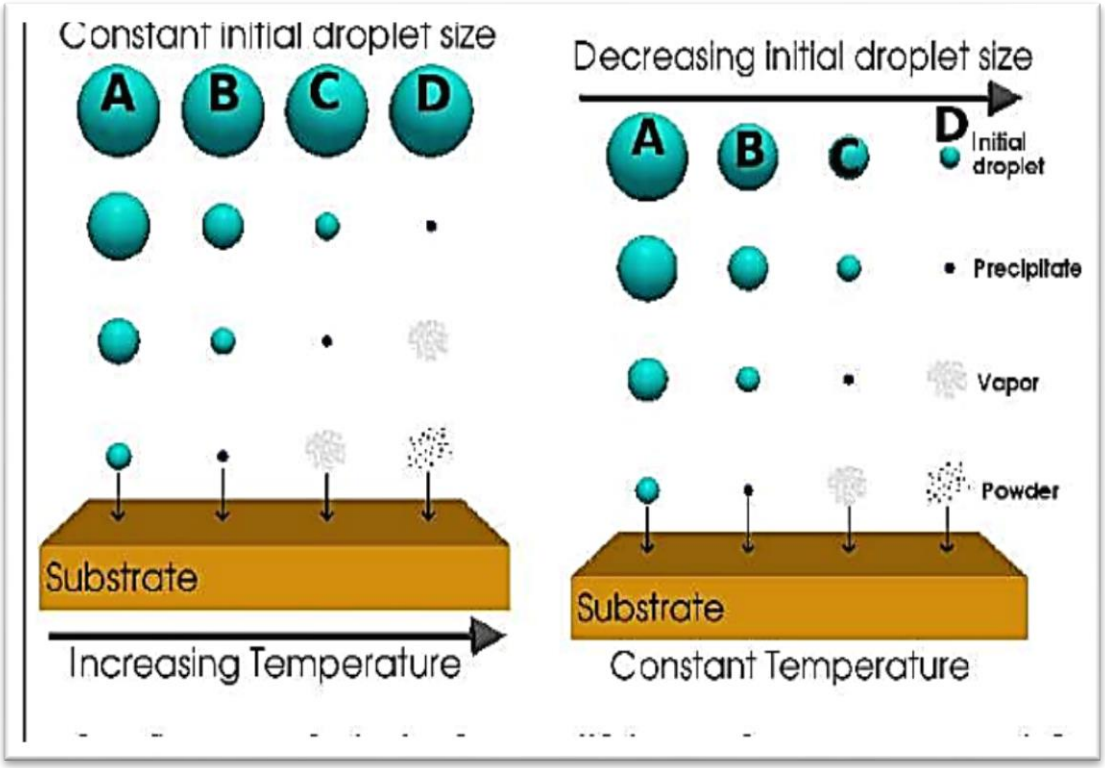

Figure (1.3): Different deposition states depending on the size of the formed droplets [14].

Case (A): In this case the size, of the drop is large, as the absorbed heat is not sufficient to evaporate the solution .When the drop collides with the substrate, a solid precipitate is formed after the solvent evaporates which leads to the large size of the drop directly affecting the temperature of the substrate, as it leads to a large and sudden decrease that leads to the possibility of breaking the substrate due to the occurrence of internal stresses that affect the properties of the film.

Case (B): This case is the ideal case for the formation of the thin film, as the ideal properties of the film are obtained, as the temperatures are between medium, and high and the droplet size is between medium and small, and the solvent evaporates shortly before reaching the substrate as the evaporated sediments undergo a chemical reaction at the point closest to the substrate.

Case (C): In this case, the droplet size is small and the temperature is high. Thus the droplets dry before reaching the base and form a dense powder. Their

adhesion force to the base is very weak i.e. they form very small granules that can be removed from the base. This case occurs when the deposition distance is large.

Case (D): The drop size is small, so the solution evaporates completely away from the substrate and the particles become small crystals that form a powder-like precipitate that clouds the film and reduces the permeability of the material, so the chemical reaction is faster than in the previous cases. The drop size has an effect on the nature of the deposited film, as the size of the drops generated from the solution is not related to the properties of the liquid, but rather depends on the density of the distribution of the drops per unit area during the deposition process. Also, the properties of the formed film, in addition to being affected by the size of the drops, are also affected by the nature and temperature of the base [15] .

1.6 Manganese Oxide

Manganese oxide (Mn_3O_4) is one of the mixed-valence oxides of manganese, and in its natural form it is known as Hausmannite. This compound exhibits distinctive physical, electrical, and optical properties. The Mn_3O_4 structure consists of a combination of manganese ions in the oxidation states +2 and +3, where Mn^{+2} ions occupy the tetrahedral (A) sites, while Mn^{+3} ions reside in the octahedral (B) sites within a spinel-type framework. Mn_3O_4 crystallizes in a distorted tetragonal spinel structure as a result of the Jahn–Teller distortion associated with the Mn^{3+} ions. The compound belongs to the space group $I4_1/amd$, with typical lattice parameters of approximately $a \approx 5.76$ Å and $c \approx 9.44$ Å. In its bulk form, Mn_3O_4 exhibits a dark brown to black coloration, a density of about 4.86 g/cm³, and a melting point near 1560 °C. From the electronic perspective, Mn_3O_4 is classified as a semiconducting material with a relatively narrow band gap in the range of 1.8–2.2 eV.

Depending on the synthesis conditions and doping, it can exhibit either n-type or p-type conductivity. In terms of morphology, bulk Mn_3O_4 crystallites adopt the tetragonal structure, whereas thin films and nanostructures prepared by chemical or physical deposition techniques often reveal diverse surface morphologies that are strongly dependent on processing parameters such as substrate temperature, deposition time, and precursor composition. The scientific and technological importance of Mn_3O_4 arises from its versatile optical, electrical, and magnetic properties, which enable its utilization in a broad range of applications including catalysis, battery electrodes, energy-storage systems, optical thin films, and magnetic micro- and nanodevices [16].

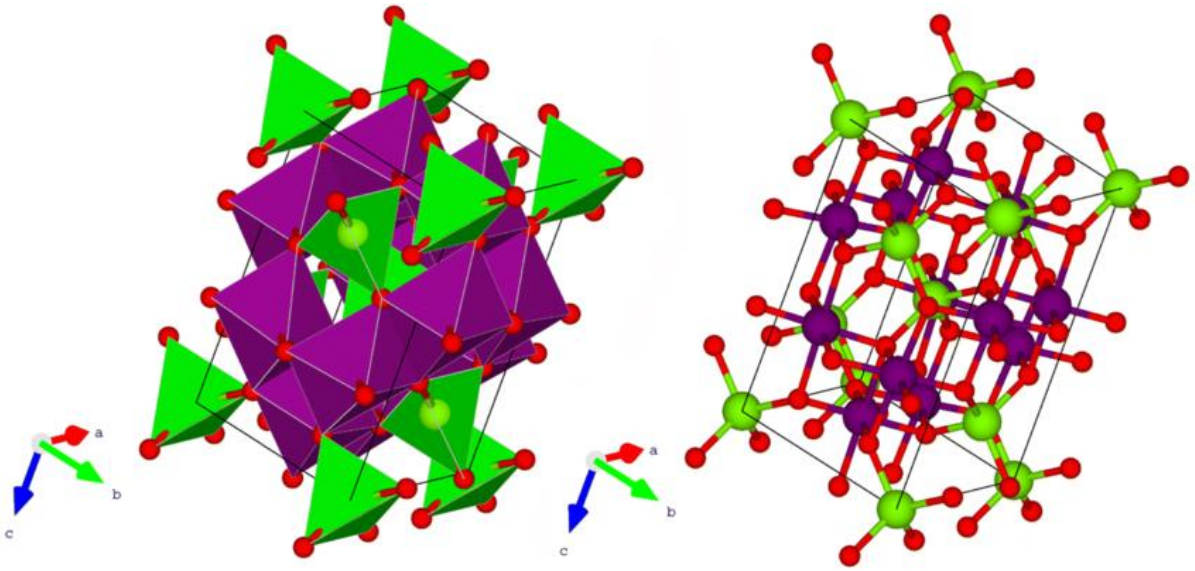

Figure (1.4): Crystal Structure of Hausmanite (Mn_3O_4) purple spheres indicate Mn at octahedral sites, green spheres indicate Mn at tetrahedral sites and red spheres are oxygen[17] .

Table (1.1) : Some physical and chemical properties of (Mn_3O_4) [16].

Sample	Crystal structure	Mollar Wight g/ml	Density g/cm^3	Melting point	Energy Gap (eV)	Color
Mn_3O_4	Tetragonal	228.81	4.86	1560 °C	1.8-2.2	**dark brown to black**

1.7 Nickel Oxide (NiO)

This is the only nickel oxide that has been well characterized. It is extremely rare to find NiO in its mineralogical form bunsenite. Numerous methods can be used to create NiO. Nickel powder reacts with oxygen when heated above 400 ^{0}C to form NiO. In certain commercial processes, nickel powder and water are heated to 1000 ^{0}C to create green nickel oxide the rate of this reaction can be improved by the addition of NiO [18]. Pyrolysis is the simplest and most efficient method of producing nickel oxide from nickel compounds, including the hydroxide, nitrate, and carbonate. This process results in a light green powder. On the other hand, heating the metal in an oxygen atmosphere to synthesize nickel oxide can produce grey to black powders, indicating nonstoichiometric [19]. Figure (1.5) illustrates how NiO takes on the NaCl structure, containing octahedral Ni^{+2} and O_2^{-2} sites. This represents the fundamental structural configuration, commonly referred to as the rock salt structure. The non-stoichiometry observed in nickel oxide induces a noticeable colour shift, wherein non-stoichiometric NiO exhibits a black appearance, while stoichiometrically precise NiO displays a green coloration. Nickel oxide (NiO) has a molecular weight of 74.69 g/mol, a density of 6.67 g/cm^3, and a melting temperature of 1955 ^{0}C. [20]. Thin coatings of nickel oxide have been used as an antiferromagnetic substance [21]. p-type transparent conducting films [22] . Electro catalysis [23]. Positive electrode in batteries[24]. Fuel cell [25]. A material for electro-chromic display devices [24]. Part of functional sensor layers in chemical sensors [26]. Solar thermal absorber[27]. Photo electrolysis

[28]. Promising ion storage material in terms of cyclic stability. Resistive memories. Electro chromic devices. Giant magneto resistive spin valve structures [29].

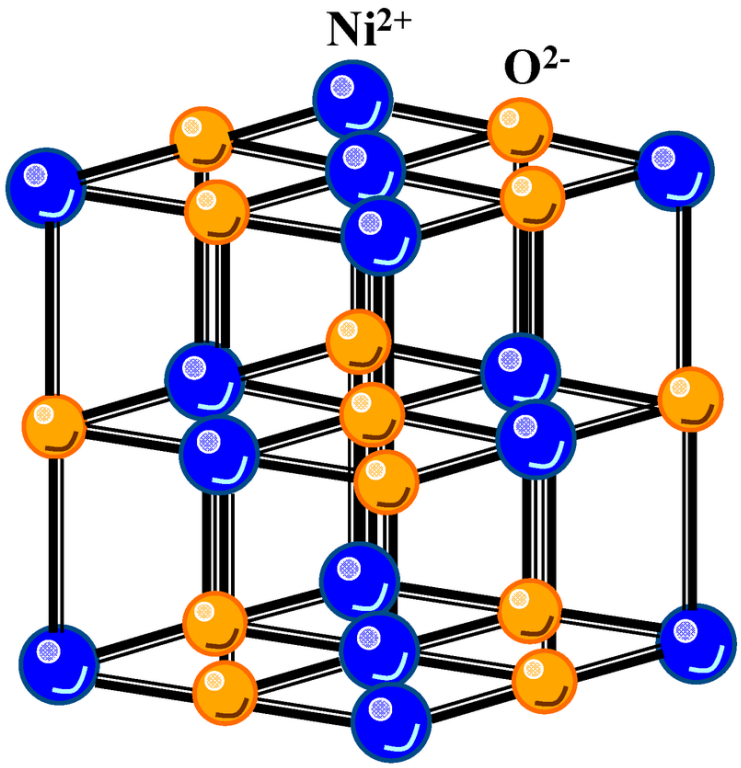

Figure (1.5): crystal structure of nickel oxide [18].

Table (1.2) : Some physical and chemical properties of (NiO) [19].

Molecular Formula	Crystal structure	Molecular Weight (g/mol)	Density (g/cm^3)	Melting Point (^0C)	Energy Gap (eV)	Colour
NiO	Cubic	74.69	6.67	1955	3.6 – 4.0	Green

1.8 Literature Review

Ubale et al. [2012] Nanostructured, nearly transparent, and conducting Mn_3O_4 thin films were deposited on glass substrates at room temperature using the SILAR technique with $MnCl_2$ and NaOH as precursors. The films were structurally and morphologically characterized by XRD, FESEM, EDX, AFM, and FTIR analyses. Optical and electrical studies revealed an optical band gap of 2.70 eV and an activation energy of 0.14 eV. Thermo-emf measurements confirmed the p-type semiconducting behavior of the Mn_3O_4 thin films [30].

Belkedkar et al. [2014] Mn_3O_4 thin films were successfully grown on glass substrates at room temperature using the SILAR method with $MnCl_2$ precursor. XRD confirmed the orthorhombic structure, while FE-SEM and FAM analyses revealed a porous nanocrystalline morphology. Optical studies showed a direct band gap of 2.70–2.68 eV, which varied with crystallite size. Electrical resistivity measurements demonstrated p-type semiconducting behavior of the SILAR-deposited films [31].

Ulutas et al. [2016] Mn_3O_4 thin films were deposited on glass substrates at 30 °C using the chemical bath deposition (CBD) method and subsequently annealed at 100–500 °C. XRD confirmed polycrystalline tetragonal structure. Optical properties, including dielectric constant (ε_1, ε_2), refractive index (n), extinction coefficient (k), and band gap, were characterized by UV–vis spectroscopy, while electrical conductivity was measured using the Hall effect, showing values of $(1.32–6.65)\times10^{-6}\ \Omega^{-1}\,cm^{-1}$ depending on annealing temperature [32].

Saidet et al. [2017] Zr-doped Mn_3O_4 thin films were deposited by spray pyrolysis with 0–20 at.% Zr. XRD, AFM, Raman, FTIR, and EDS analyses confirmed tetragonal hausmannite spinel structure. Increasing Zr content

reduced crystallite size (~24.1 nm at 20 at.% Zr), enhancing gas adsorption, and widened the optical band gap (2.92–6 eV), indicating improved optical and surface properties for sensor applications. [33] .

Bayram et al. [2018] Nanostructured Cu-doped Mn_3O_4 thin films were successfully deposited using the SILAR technique. Characterization by SEM, XRD, and UV–Vis spectroscopy confirmed that Cu doping induced a porous morphology, modified the crystal structure, and reduced the band gap from 2.06 to 1.71 eV, while influencing the dielectric constant, refractive index, and extinction coefficient, demonstrating controllable structural and optical properties through Cu incorporation [34] .

Kocyigitet et al.[2018] Mn_3O_4 and Mn_3O_4/Au composite thin films were deposited by spray pyrolysis to study their structural, optical, and electrical properties. XRD showed an amorphous structure for Mn_3O_4 and a crystalline structure for the Mn_3O_4/Au composite. UV–Vis analysis revealed that Au incorporation reduced the band gap and transmittance, while SEM showed improved morphology. EDS confirmed successful composite formation, and sheet resistance decreased with Au addition, indicating potential applications in supercapacitors and sensors [35].

Fauzin et al.[2019] Hausmannite (Mn_3O_4) thin films were prepared by the sol–gel spin coating method using sintered and milled manganese ore. The films were calcined at 200, 300, 400, and 500 °C. XRD analysis revealed the formation of Mn_3O_4 and Mn_2O_3 phases, with crystallite sizes of 41.06, 52.37, 47.73, and 47.87 nm, respectively, depending on the calcination temperatur[36].

Bayram et al.[2019] Researchers deposited cobalt-doped Mn_3O_4 thin films on soda-lime glass substrates using the SILAR method. They characterized the films using XRD, SEM, UV–Vis, and Raman spectroscopy and found that the films exhibited a Hausmannite crystal structure. Increasing

Co concentration shifted the preferred orientation from (002) in pure and 0.5 at.% Co-doped films to (211). UV–Vis analysis showed that Co doping initially increased the optical band gap (2.00 eV for pure Mn_3O_4) and significantly affected the transmittance (60–70%) and absorbance [37].

Nkele et al. [2020] Researchers synthesized Mn_3O_4 thin films and Mn_3O_4-decorated graphene films using the SILAR method. They characterized the films with UV–Vis spectroscopy, XRD, EDS, and SEM, and found that decorating Mn_3O_4 on graphene transformed the structure from amorphous to crystalline and produced fused capsule-like nanoparticles. EDS confirmed the elemental composition, while optical measurements showed enhanced transmittance and band gap. The decorated films demonstrated improved structural, optical, morphological, and electrochemical properties, indicating their potential for optical and electrochemical devices [38].

Xaba and Shooto et at. [2021] Researchers deposited Mn_3O_4 nanocrystalline thin films on silicon and glass substrates using the spin-coating method and investigated the effect of annealing temperature. XRD confirmed tetragonal phase formation (a = b = 5.75 Å, c = 9.44 Å), while SEM showed improved surface crystallinity at higher temperatures. Optical measurements revealed that increasing the annealing temperature caused a redshift in absorption and emission spectra and a decrease in band gap energies [39].

Shano et al.[2021] Researchers deposited Mn_3O_4 nanostructured thin films of varying thicknesses (200–350 nm) on glass substrates using chemical spray pyrolysis at 400 °C. XRD confirmed polycrystalline tetragonal structure with (211) preferential orientation, and crystallite size decreased with increasing thickness. UV–Vis spectroscopy showed that the optical band gap decreased as thickness increased, while the absorption coefficient, dielectric constant, and extinction coefficient varied with photon energy [40] .

Rossi et al.[2022] Researchers deposited NiO thin films on silicon substrates using co-deposition and pulsed sputtering techniques to fabricate a UV photodetector. They characterized the films' structural, optical, and electrical properties and found that the films exhibited high crystallinity. Increasing the laser intensity enhanced the spectral response from 2.7 to 3.7 μA/mW, indicating improved photodetection performance[41].

Rossi et al.[2023] Researchers prepared pure Mn_3O_4 and Sn-doped Mn_3O_4 thin films on glass substrates at 350 °C using chemical spray decomposition. XRD confirmed polycrystalline tetragonal structure, EDS verified composition, and FE-SEM revealed surface topography. Optical analysis showed that transmittance increased (57.6–62.2 %) with wavelength, the band gap widened (3.27–3.61 eV), dispersion energy (E_ed) decreased (5.44–4.86 eV), and the static refractive index (n_0) decreased (2.02–1.86), indicating suitability for nonlinear optical applications [42].

Obaid et al.[2023] Researchers deposited GeO_2-doped SnO_2 thin films on silicon substrates using co-deposition and pulsed deposition to fabricate a UV photodetector. XRD and FE-SEM confirmed high crystallinity and film thickness of 50–85 nm. Optical analysis showed a band gap of 3.8–4.2 eV, and the doped films exhibited a photocurrent of 148 μA at 396 nm, indicating enhanced UV detection performance [43].

Patil et al.[2024] We deposited Mn_3O_4 thin films by a simple electrophoretic technique using $MnSO_4$ precursors with different molarities (0.05–0.125 M). We investigated how precursor concentration affects the films' structure, morphology, optical response, and supercapacitive behavior. The nanocrystalline tetragonal films exhibited porous morphologies (nanowires/nanoflowers) with a preferred (220) orientation. Electrochemical testing confirmed their pseudocapacitive nature, with the film grown at 0.05 M

showing the best performance, delivering 237 F g^{-1} and retaining 70% of capacitance after 2000 cycles. These findings demonstrate the strong potential of nanostructured Mn_3O_4 thin films as electrode materials for supercapacitor applications.[44]

Doroudkhani et at [2025] NiO: Mn_3O_4 ribbons were synthesized via electro spinning and compared with NiO nanoparticles and Mn_3O_4 octahedral particles to investigate their optical and electrochemical properties. XRD confirmed the coexistence of cubic NiO and tetragonal Mn_3O_4 phases within the nanostructure. UV–Vis DRS revealed a bandgap of 3.53 eV, while photoluminescence quenching indicated enhanced surface defects. The ribbons delivered a high specific capacitance of 372 F. Moreover, the NiO: Mn_3O_4/AC asymmetric superc apacitor achieved an energy density of 40 Wh kg^{-1}. These results highlight the potential of NiO–Mn_3O_4 ribbons for high-performance thin-film-based energy storage devices [45] .

1.9 Aim of the Study

This study aims to:

1. A photo detector within the visible spectral range was successfully fabricated by the deposition of pure manganese oxide (Mn_3O_4) and nickel-doped manganese oxide (Mn_3O_4:Ni) thin films onto silicon substrates.

2. Thin films of manganese oxide pure (Mn_3O_4) doped with nickel oxide (NiO) with different doping ratios (0,1,3,5, and 7%) were prepared by depositing them on glass substrates at a temperature (350 ^{0}C) using the chemical spray pyrolysis deposition technique.

3. Study the effect of changing the nickel oxide doping ratios on the some properties of the prepared films.

الخلاصة

في هذه الدراسة تم تحضير أغشية رقيقة من أوكسيد المنغنيز (Mn_3O_4) المشوب بألنيكل بنسب تشويب مختلفة (0،1،3،5، و7%) وذلك بترسيبها على ركائز زجاجية عند درجة حرارة (350 درجة سيليزية) وبسمك (327) نانومتر باستخدام تقنية التحلل الحراري الكيميائي (CSP) .

تمت دراسة تأثير تغيير نسب التشويب بالنيكل على الخصائص البنيوية والبصرية والكهربائية للأغشية المحضرة باستعمال حيود الأشعة السينية(XRD)، ومجهر القوة الذرية(AFM) ، والمجهرالإلكتروني الماسح الباعث للمجال (FE-SEM)، ومطيافية الأشعة فوق البنفسجية والمرئية وتأثير هول.

أظهرت نتائج فحوصات الأشعة السينية أن جميع الأغشية المُحضرة بنسب تشويب مختلفة لها بنية متعددة البلورات من النوع الرباعي، وأن اتجاه النمو السائد لجميع الأغشية هو (101). وُجد أن الحجم البلوري يتناقص مع زيادة نسب التشويب. كما تم حساب قيم ثوابت الشبيكة، وعدد البلوريات في وحدة المساحة، وكثافة الخلاعات.

أظهرت نتائج مجهر (AFM) انخفاضًا في متوسط خشونة المربع وخشونة السطح مع زيادة نسبة التشويب النيكل.

وكشفت دراسات المجهر الإلكتروني الماسح الباعث للمجال (FE-SEM) أن الأغشية الناتجة لها أسطح ذات تراكيب كروية متجمعة على شكل زهرة، تشبه إلى حد كبير زهرة القرنبيط. ومع ذلك، يتناقص متوسط حجم الحبيبات مع زيادة نسبة التشويب النيكل .

دُرست الخصائص البصرية لجميع الأغشية المُحضرة لجميع نسب التشويب، وذلك بتسجيل أطياف النفاذية والامتصاصية عند أطوال موجية تتراوح بين (300-1100) نانومتر. وأظهرت النتائج أن فجوة الطاقة البصرية للانتقال الإلكتروني المباشر المسموح به في الأغشية المُنتجة تتراوح بين (2.65-2.95) إلكترون فولت. ونلاحظ أن قيم النفاذية تزداد، بينما تنخفض الامتصاصية بزيادة نسب التشويب. وقد حُسبت قيم الثوابت البصرية لجميع الأغشية المُحضرة، والتي تشمل (معامل الامتصاص، ومعامل الانكسار، ومعامل الخمود، وثابت العزل الحقيقي والخيالي) كدالة لطاقة الفوتون.

أظهرت الأغشية الرقيقة الناتجة (Mn_3O_4) المشوبة بالنيكل بجميع نسب التشويب موصلية كهربائية من النوع p ، كما ثبت من خلال الاختبارات الكهربائية باستعمال تأثير هول. ويعود ذلك إلى انخفاض موصلية الأغشية ومقاومتها العالية.

دُرست خصائص الكاشف المُحضّر بترسيب أغشية (Mn_3O_4) والمُشَوَّبة بالنيكل عند درجة حرارة (350) درجة سيليزية، ومُرسَبة على ركائزمن سليكون. أظهرت نتائج قياسات التيار والجهد أن

الكاشف المُحضّر من نوع (غير متماثل)، وأن تيار الظلام وتيار الاضاءة تزداد بزيادة نسب التشويب في حالة الانحياز الأمامي. أما في حالة الانحياز العكسي، فينخفض التيار الناتج بزيادة نسب التشويب.

دُرست معاملات الكاشف، اذ أظهرت الاستجابة الطيفية تزايدًا مع زيادة نسب التشويب، وكانت أعلى قيمة لها عند الأطوال الموجية القصيرة وفي الحالة النقية. وأظهرت نتائج الكشف البصري انخفاضًا مع زيادة نسب التشويب، وكانت أعلى قيمة لها عند الأطوال الموجية القصيرة. وأظهرت نتائج الكفاءة الكمية الخارجية زيادةً مع زيادة نسب التشويب، وكانت أعلى قيمة لها عند الحالة النقية وعند الأطوال الموجية القصيرة .

جمهورية العراق
وزارة التعليم العالي والبحث العلمي
جامعة ديالى
كلية العلوم
قسم الفيزياء

تحضير ودراسة بعض الخصائص الفيزيائية لأغشية أوكسيد المنغنيز المطعم بالنيكل لتطبيق الكواشف الضوئية

رسالة مقدمة إلى

مجلس كلية العلوم- جامعة ديالى ، وهي جزء من متطلبات نيل درجة الماجستير في علوم الفيزياء

مقدمة من

علي يونس ابراهيم

(بكالوريوس علوم فيزياء ٢٠١٩)

بأشراف

الاستاذ المساعد الدكتور

فيصل غازي حمودي

١٤٤٧ هـ ٢٠٢٥ م